

# **Porous titanium-hydroxyapatite composite coating obtained by cold gas spray improves osteoblast cell response on titanium**

J. Guillem-Martí<sup>a,b</sup>, N. Cinca<sup>c</sup>, M. Punset<sup>a,b,d</sup>, I.G. Cano<sup>c</sup>, F.J. Gil<sup>a,e</sup>, M.-P. Ginebra<sup>a,b,f</sup>, J.M. Guilemany<sup>c</sup>, S.Dosta<sup>c,\*</sup>

<sup>a</sup>*Biomaterials, Biomechanics and Tissue Engineering group, Department of Materials Science and Metallurgical Engineering, Universitat Politècnica de Catalunya (UPC), 08930 Barcelona, Spain.*

<sup>b</sup>*Barcelona Research Center in Multiscale Science and Engineering, Universitat Politècnica de Catalunya (UPC), 08930 Barcelona, Spain*

<sup>c</sup>*Centre de Projectió Tèrmica (CPT). Departament de Ciència dels Materials i Enginyeria Metal·lúrgica. Universitat de Barcelona (UB), 08028 Barcelona, Spain.*

<sup>d</sup>*UPC Innovation and Technology Center (CIT-UPC), 08028 Barcelona, Spain.*

<sup>e</sup>*Universitat Internacional de Catalunya (UIC), 08195 Sant Cugat del Vallès, Spain.*

<sup>f</sup>*Institute for Bioengineering of Catalonia (IBEC), Barcelona Institute of Technology (BIST), 08028 Barcelona, Spain*

*\* Corresponding author at:*

*Thermal Spray Center (CPT). Dpt. Ciència dels Materials i Enginyeria Metal·lúrgica, Universitat de Barcelona, Barcelona, Spain*

*E-mail address: [sdosta@cptub.eu](mailto:sdosta@cptub.eu)*

## **Abstract**

The lack of bioactivity of titanium (Ti) is one of the main drawbacks for its application in biomedical implants since it can considerably reduce its osseointegration capacities. One strategy to overcome this limitation is the coating of Ti with hydroxyapatite (HA), which presents similar chemical composition than bone. Nonetheless, most of the strategies currently used generate a non-stable coating and may produce the formation of amorphous phases due to the high temperatures used. Herein, we propose to generate an HA coating on Ti surface mixing HA with Ti to improve the stability of the bioactive coating. The coating was performed under low temperature by cold gas spraying and was thoroughly characterized. The novel Ti-HA coating presented high porosity and high adhesion and bond strengths. In addition, no change in HA phases was observed after coating formation. Moreover, osteoblast-like cells adhered, proliferated and differentiated on Ti-HA coated surfaces suggesting that the novel coating might be a good candidate for biomedical applications.

**Keywords:** Titanium, Hydroxyapatite coating, bioactivity, Cold gas spray, osteoblast-like cells.

## **1. Introduction**

Although life expectancy has exponentially increased over the last decades, organ failure and traumatic injuries considerably decrease the quality of life of older people. For instance, more than one million patients worldwide undergo annually to total hip arthroplasty (THA) or total knee arthroplasty (TKA) surgery [1]. By 2030, based on the data collected on total joint replacement surgery, the demand for THAs and TKAs is estimated to grow reaching 4 million procedures per year only in USA [2]. Therefore, there is a need to develop new long lasting orthopedic prostheses, either with new designs and/or new materials, with higher reliable performance with the aim to improve their long-term success rates.

Titanium (Ti) has long been used for biomedical applications due to its excellent resistance to corrosion, biocompatibility, good mechanical properties and osteoconductivity [3]. However, titanium implants still present some limitations that may pose concerns in clinical practice, mainly due to its bioinert nature, i.e. lack of bioactivity [4]. Several strategies are being used to improve the bioactivity of Ti including surface roughening at the micro- and nanoscale level by mechanical or acid/alkali treatments, or biochemical coating techniques [5,6]. In this latter regard, hydroxyapatite (HA) coatings on Ti result in enhanced bone formation and improved fixation to adjacent bone compared to uncoated Ti [7]. However, the long-term stability of the HA coated devices is still controversial mainly due to the unsatisfactory bonding strength between coating/substrate interface limiting their clinical applications [8].

There are several methods being used for the generation of HA coatings, which can be grouped into two main strategies reviewed in [7]: physical deposition and wet-chemical techniques. Wet-chemical techniques are biomimetic coating processes based on the induction of calcium phosphate nucleation at material surfaces through immersion of

biomaterial in a supersaturated calcium phosphate solution [9], including deposition processes such as dip coating [10], sol-gel [11], electrophoretic [12] and aerosol [13], among others. Although this allows the immobilization of biofunctional cues, the calcium phosphate layer dimensions are difficult to control and are mainly composed of low-crystalline apatite [14]. Physical deposition processes include many different approaches as sputtering [15], ion-beam assisted deposition [16] and pulsed laser ablation [17], but most of them are based on thermal spray processes [18]. HA coatings on metallic implants have been produced by several plasma spray (PS) techniques including atmosphere (APS) [19], suspension (SPS) [20], controlled atmosphere (CAPS) [21], vacuum (VPS) [22], high velocity oxygen fuel (HVOF) [23], liquid precursor (LPPS) [24], low-pressure (LPPS) [25] and high velocity suspension flame spraying (HVSFS) [18]. Despite this versatility, only PS processes are actually approved by the FDA to produce HA biomedical coatings.

Nonetheless, due to extremely high working temperatures, physical deposition methods usually induce the formation of amorphous phases at the implant-coating interface, which have high dissolution rates in contact with body fluids. This HA phase transitions may reduce bonding strength between HA and Ti and also may lead to undesired biological responses related to HA particulate debris that may eventually lead to implant failure, mainly through inflammatory reactions [26,27].

Another strategy that is well accepted by the FDA is the use of porous rough titanium coatings, a Ti plasma-sprayed (TPS) coating that is engineered to have a greater surface roughness and larger pore size, promoting bone growth into and around the implant. Porous rough TPS coatings still have all the qualities of a standard PS titanium coating, such as bio-inertness, bio-compatibility, and the ability to coat dissimilar substrates [28].

However, the use of PS technology for the production of such coatings implies costly vacuum installations in order to avoid titanium oxidation.

An interesting alternative is the use of Cold Gas Spraying (CGS) technique [29]. Very few attempts have been performed to produce pure HA coatings by CGS due to the difficulties for cohesion among ceramic particles. Therefore, a ductile phase can be used to generate composite coatings. Some works deal with Ti-HA mixtures, even achieving a better bond strength (24.45MPa) than APS (10-15MPa) [30]. The HA particles usually appear exposed at the surface of the coating, resulting in enhanced mineralization ability [31], higher corrosion current and lower corrosion resistance, and better bonding strength (25 MPa) compared to pure HA coating [32]. However, the mechanical stability of those coatings could still be a problem either for surgical operation or after implantation. In a previous study by our group, Ti-HA composite coatings with promising bonding strength (60 MPa) were obtained through CGS [33].

The aim of this study was to bioactivate Ti surface producing a high bonding strength HA coating. To this end, a 70%Ti-30%HA composite coating was obtained by CGS in order to prevent HA phase transformation. The coating was thoroughly characterized and was compared to a Ti coating also performed by CGS. Moreover, biological response was evaluated by means of adhesion, proliferation and differentiation of osteoblast-like cells to assess the biocompatibility of the coating and the feasibility for its application to biomedical implants.

## **2. Materials and Methods**

### **2.1. Coating production and structural characterization**

Commercially pure (c.p.) titanium powder was supplied by GfE (Gesellschaft für Elektrometallurgie, Germany) with a particle size distribution of  $90 \pm 22 \mu\text{m}$ . The HA powder was provided by Plasma Biotal (Captal 30) (Tideswell, United Kingdom) with a

particle size distribution of  $-50 +10 \mu\text{m}$ . Both pure Ti and Ti-HA blends were sprayed at the same previously defined parameters [32]. The blend ratio of the two powders for spraying was 70%Ti-30%HA (v/v). A high pressure KINETICS® 4000 CGS thermal spraying Gun with N<sub>2</sub> as propelling gas was used to spray coatings, with maximum gas pressure of 40 bars and a maximum gas temperature of 800°C.

The coating was characterized using a JEOL 5320 Scanning Electron microscope (SEM) and FESEM JEOL J-7100 operating at 15KeV. Microstructure analyses were performed following ASTM E3-01 [34], consisting of embedding samples in resin for grinding with different SiC papers and finally polished using 1 $\mu\text{m}$  alumina abrasive suspension. Samples were chemically etched in 100 ml H<sub>2</sub>O, 5 ml HF and 2 ml H<sub>2</sub>O<sub>2</sub> solution and microstructure was observed using a DM5000M optical microscope (Leica, Germany). For the study of the topography, the roughness values were measured with a *Map DCM 3D* confocal microscope (Leica).

Micro- and macro-porosity were evaluated by mercury intrusion porosimetry (MIP) using an AutoPore IV 9500 V1.07 equipment (Micrometrics, USA). Analysis was performed to determine pore entrance size distribution (PESD) within the material. Moreover, open macroporosity was evaluated for pore diameters greater than 10 $\mu\text{m}$ .

Siemens D500 X-ray diffraction Bragg–Brentano type  $\theta/2\theta$  apparatus, with Cu K $\alpha$ 1 + 2 radiation with  $\alpha_1 = 1.54060$  and  $\alpha_2 = 1.54443$  at 40 kV and 30 mA, was used to analyze the purity, crystallinity, phase composition and residual stress state of both types of feedstock powders as well as of both types of coatings (Ti and Ti-HA coatings).

## **2.2 Ion release**

Ti-HA coatings were immersed in simulated body fluid (SBF) Hank's solution to understand physiological interactions between the implant and the surrounding environment. Since Ca is one of the main ions that contribute to the osseointegration

between the prosthesis and bone, an Inductively Coupled Plasma (ICP) technique was used for determining Ca concentration after 1, 4 and 7 days of immersion in Hank's solution.

## **2.2 Mechanical Characterization**

The adhesion strength of coatings was measured according to ASTM standard C633-13 [35] at atmospheric temperature on the Ti and Ti-HA CGS coatings glued to uncoated sand-blasted specimens using F1000 glue. Mechanical testing was done in a tensile loading machine with self-aligning devices at  $0,025 \text{ mm}\cdot\text{min}^{-1}$  of displacement rate. For each coating type, the adhesion of five test pieces was measured in order to ensure a statistically representative average value.

## **2.3. Biological characterization**

### *2.3.1 Cell culture*

Human osteoblast-like SaOS-2 cells (ATCC, USA) were cultured in McCoy's 5A medium (Sigma-Aldrich, USA) supplemented with 10% fetal bovine serum (FBS), 2 mM L-glutamine, 2 mM sodium pyruvate, penicillin/streptomycin ( $50 \text{ U ml}^{-1}$  and  $50 \mu\text{g ml}^{-1}$ , respectively) and 20 mM HEPES buffer solution (all from Invitrogen, USA) at  $37^\circ\text{C}$  with 5%  $\text{CO}_2$  in a humidified atmosphere. Medium was changed every two days and subconfluent cells were trypsinized using TrypLE solution (Invitrogen). Cells were seeded at a density of  $10 \times 10^3$  cells/sample in each of the following experiments.

### *2.3.2. Cytotoxicity*

Cytotoxicity tests were performed following the ISO 10993-5 standard [36]. Briefly, samples were incubated for 72 h at  $37^\circ\text{C}$  in complete medium and supernatants were collected. Serial dilutions of these extracts in complete medium (Non-dilution, 1:1, 1:10, 1:100, 1:1000) were transferred to new microplate wells containing adhered SaOS-2 cells (10.000 cells). Afterwards, cells were incubated for 24 h, washed with phosphate-

buffered saline (PBS) and lysed with 100 µl of M-PER (Mammalian Protein Extraction Reagent; Thermo Scientific, USA). Viable cells were quantified measuring the enzymatic activity of lactate dehydrogenase (LDH) using the Cytotoxicity Detection Kit<sup>PLUS</sup> LDH (Roche Applied Sciences, Germany). The enzymatic activity was measured spectrophotometrically at 492 nm in a PowerWave HT microplate reader (Bio-Tek, USA) and the percentage of cell viability was calculated following the guidelines of the kit.

### *2.3.3. Cell morphology*

Cells were seeded on samples and allowed to adhere for 6h. Then, cells were washed in 0.1 M phosphate buffer (PB) and fixed with 2.5% glutaraldehyde solution in PB for 1 h. Afterwards, samples were washed thrice in PB and dehydrated in ethanol. Complete dehydration was performed in hexamethyldisilazane (HMDS) for 15 min and samples were dry stored in a dessicator. Samples were covered with a thin carbon layer and visualized with a FESEM JEOL J-7100 (JEOL Ltd., Japan) at an operating voltage of 15 kV.

### *2.3.4. Cell proliferation*

Cells were seeded and after 6 h, 3 days, 7 days, 14 days and 21 days samples were rinsed in PBS and lysed with 300 µl of M-PER. The LDH enzymatic activity of cells at each specified time was measured using the Cytotoxicity Detection Kit<sup>PLUS</sup>. The number of cells was quantified using a calibration curve with increasing number of cells. Tissue culture polystyrene (TCPS) was used as control.

### *2.3.5. Cell differentiation*

The alkaline phosphatase (ALP) activity was quantified using the same cell lysates obtained in the cell proliferation assay. ALP activity was measured using the SensoLyte pNPP Alkaline Phosphatase Assay Kit (AnaSpec Inc., USA). Reactions were incubated at 37°C and absorbances were acquired at 405 nm using a PowerWave HT Microplate



reader (Bio-Tek). A calibration curve was performed using purified ALP provided by the kit. Results were normalized versus their corresponding cell numbers obtained in the proliferation assay and the time of incubation.

#### **2.4. Statistical analysis**

All the experiments were performed in triplicate. Data were expressed as mean values  $\pm$  standard error of the mean. Non-parametric Kruskal-Wallis tests followed by Mann-Whitney tests with Bonferroni correction were used to determine statistical significant ( $p < 0.05$ ) differences between the means of the different groups.

### **3. Results and discussion**

#### **3.1. Microstructural characterization of the coating**

Figure 1a and 1b shows a general optical micrograph of the cross section of the Ti and Ti-HA coatings with inner porosity, respectively. The average Ti-HA coating thickness was  $596 \pm 74 \mu\text{m}$ . Ti-HA interfaces are rather smooth without gaps; a nice bonding is produced as observed.

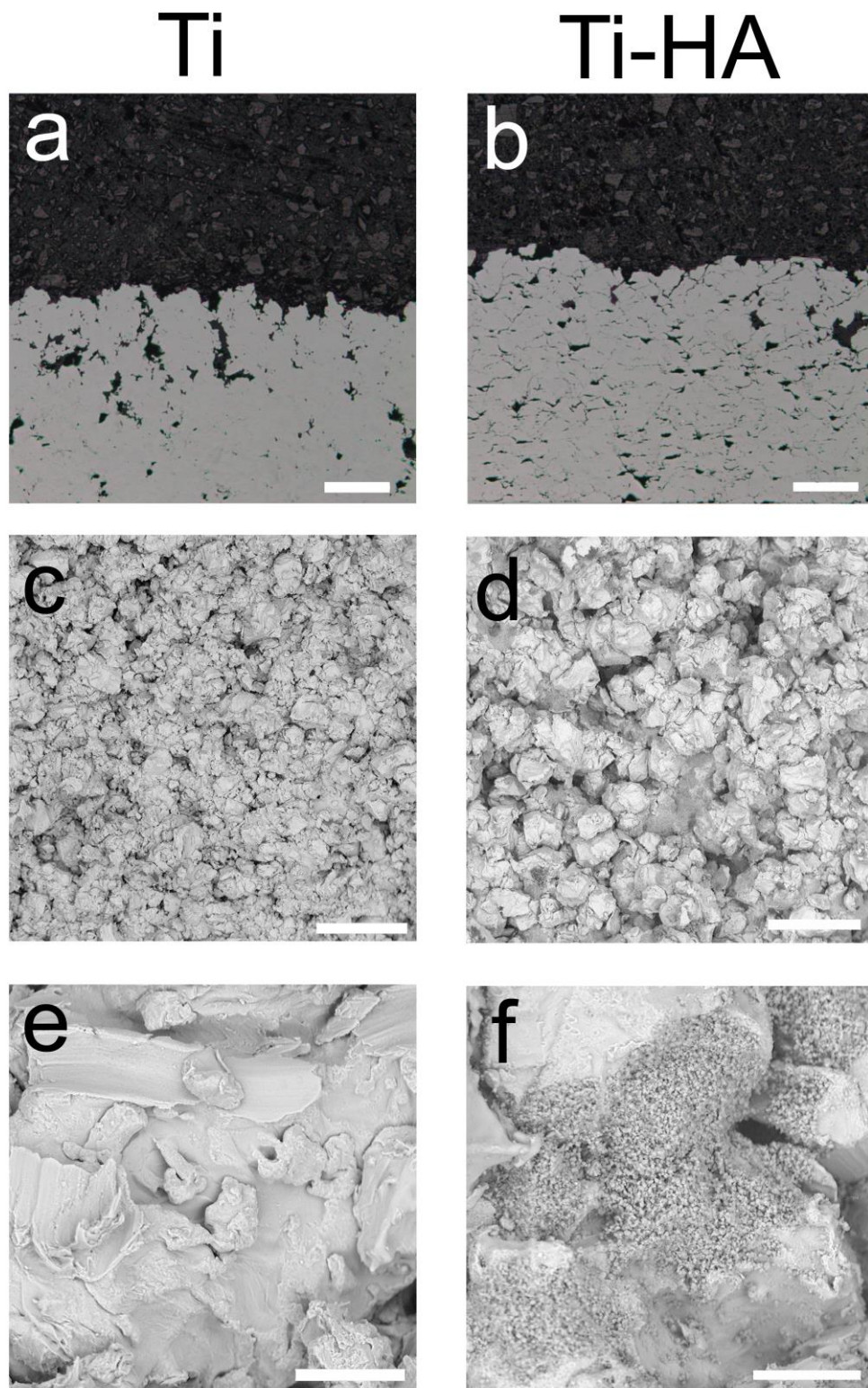


**Figure 1:** Morphology of the Ti (a,c,e) and Ti-HA (b,d,f) coatings. Cross-sectional optical micrographs (a,b) and low magnification (c,d; 300x) and high magnification (e,f; 3500x) SEM images. Scale bar denotes 200  $\mu\text{m}$  (a,b,c,d) or 20  $\mu\text{m}$  (e,f).

Noteworthy HA particles were detected over the top surface and through the entire thickness of coatings, as well as over the entire inner surface of the pores. Further examination clearly shows the preferential location of the HA particles inside the grain boundaries formed between adjacent Ti sprayed particles (Figure 1c and 1d). Although this particularity may appear detrimental for both mechanical resistance and adhesion of coatings under mechanical loading, could become a crucial factor to stimulate bone tissue ingrowth inside the porous coating.

A considerable amount of craters was found over the surface of the Ti-HA coatings mainly caused by the impacting HA particles and their subsequent detachment compared to Ti coated surfaces (Figure 1e and 1f). Further examination of the Ti-HA coating transversal section has shown the presence of a porosity gradient growing from the coating/substrate interface to the coating top surface. The typical inner inter-splat porosity showed inside the metallic Ti sprayed coatings was filled by the HA particles in the composite Ti-HA coatings, assuring the mechanical embedding of the HA particles between the deformed Ti spread particles as well as producing an interconnected mesh-like porosity paths. There were no cracks, pores or any kind of defects near coating/substrate interface, reflecting a good quality of sprayed coating.

### **3.2. Topographic surface characterization**

The top surface of the Ti-HA coating is characterized by the presence of deep wells, where hydroxyapatite is preferentially/usually found at the bottom. The sintered feedstock particles have fractured and the crystallites have scattered, typical in CGS coatings that has been explained in a previous work by our group [33]. At much higher energetic conditions, typical for spraying Ti, the presence of the wells was more dispersed and non-uniform, while at lower temperature conditions, to which hydroxyapatite had

been previously sprayed, there was no proper deposition at all. Therefore, an intermediate set-up of spraying conditions was selected as optimal for the deposition of this blend.

The synergic combination of high surface waviness with open macroporosity over the top surface of the coating is considerable beneficial from the mechanical stabilization point of view. The presence of an open surface macroporosity as well as inner porosity should also be beneficial in terms of mechanical interlocking and bone ingrowth, leading to new bone tissue ingrowth with optimal vascularization after implantation of devices.

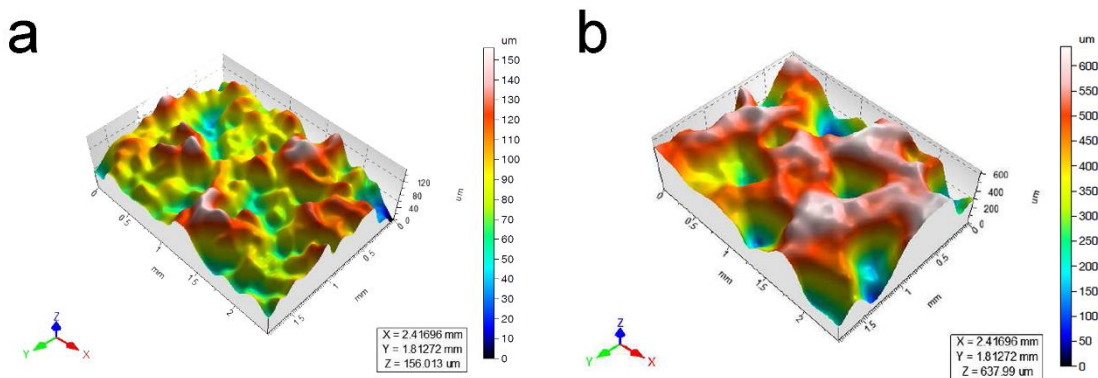


**Figure 2.** Representative White light interferometer 3D-reconstructed micrographs of Ti coating (a) and Ti-HA composite coating (b).

From Figure 2, it can be observed that the coating surfaces were characterized by a micro-roughness and submicro-roughness profile. The numerical results presented in Table 1 indicated that the waviness and roughness contribution was much higher in the composite Ti-HA coating than in the Ti coating. The average values of the Ti-HA composite presented by Ra, related to the 2D profile of the microroughness topography, double those without hydroxyapatite and the Wa was more than three times higher. Such differences, also exhibited in Rz and Wz values were the result of the HA influence.

**Table 1. Roughness parameters obtained by confocal microscopy of the as-sprayed CGS coatings.**

		<b>Ti</b>	<b>Ti-HA composite</b>
<b>Waviness 3D</b>	Sa	17	27
	Sz	406	768
<b>Waviness 2D</b>	Wa	19	65
	Wz	31	126
<b>Microroughness 2D</b>	Ra	10	25
	Rz	73	201

### **3.3. Physical characterization**

Figure 3 shows the pore size distribution curves obtained by MIP for both Ti and Ti-HA coatings sprayed by CGS methodology. It is worth noticing that the void associated to the surface macroporous crater-like geometry was mainly measured in the first step of Hg intrusion, while intergranular porosity was measured under greater pressures. The total porosity and the pore average size were smaller for the Ti coating than for Ti-HA coating. This result confirmed that higher packing density of the splat structure was obtained compared to the single-phase metallic of the Ti coating.

During the CGS progress, the total porosity and the pore size progressively increased from the substrate/coating interface to the coating top surface. This behavior may be attributed to two main reasons: the pore coarsening effect and the consequent masking effect [37], as well as the progressive reduction of base material density with the consequent loss of compaction effect in the latest films sprayed. This process resulted in the aforementioned high roughness and open crater-like porosity on the surface.

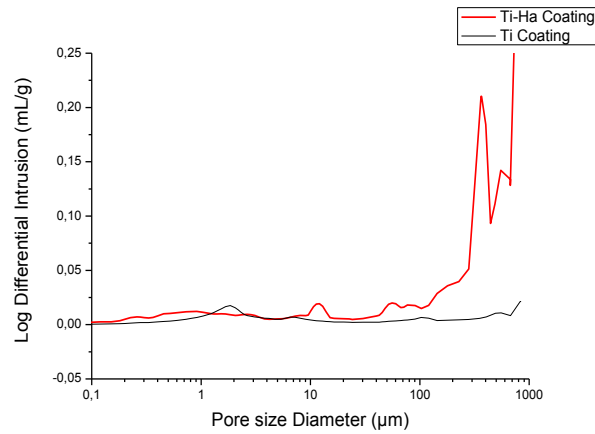


**Figure 3.** Pore diameter size distribution vs Log Differential intrusion of Ti and Ti/HA CS Coatings.

One of the main concerns of coated prostheses is the poor adherence of the HA plasma coating which may lead to failure causing severe problems for the patient. For instance, TS ceramic coatings based on HA or HA/TiO<sub>2</sub> has dealt with this issue, limiting its commercial use [38–40]. In the present study the addition of Ti to HA slightly enhanced the adhesion of the coating to the substrate without reflecting loss in the bonding strength (Figure 4). However, the values of both Ti and Ti-HA coatings were very similar ( $60 \pm 3$  MPa and  $65 \pm 4$  MPa, respectively). Tensile adhesion tests of Ti-HA coatings showed promising mechanical properties for clinical applications being higher compared to the Plasma Spraying coatings with FDA certification.

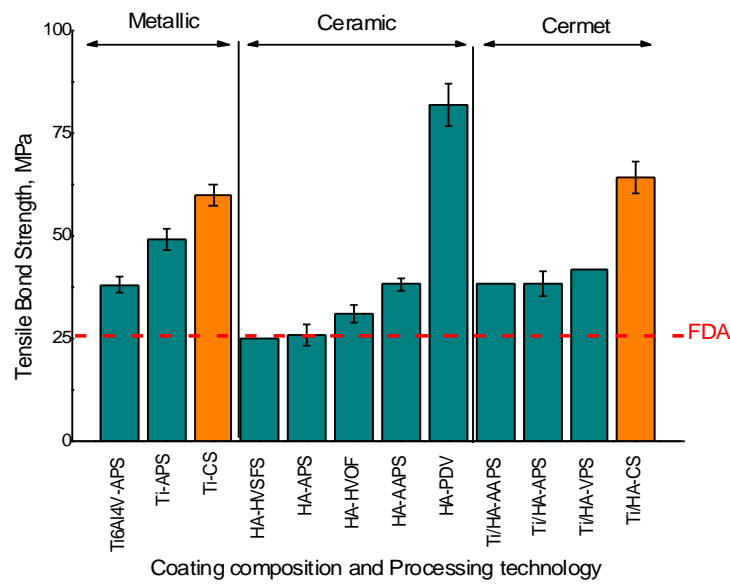


**Figure 4.** Tensile Bond strength values of coatings (metallic, ceramic and cermet) produced by different technologies including the CGS coatings produced in this study (highlighted in orange). Values in green were obtained from the literature [18,23,41–45].

Adhesion values obtained by Ti-HA composite coatings deposited by CGS showed higher values than those obtained by ceramic HA coatings deposited by other thermal spray processes, such as APS (from 5 GPa to 23 MPa) [46,47], AAPS (26,7±1,7) [48], HVOF (24±8 MPa and 31±2) [49] or HVSFS (25 MPa) [18]. Furthermore, cold sprayed Ti-HA composite coatings showed higher adhesion values than Ti6Al4V and Ti metallic coatings deposited by APS (with values up to 38 MPa) [41,47,50].

In addition, the adhesion values obtained in the present study were also significantly higher than other Ti-HA coatings deposited by thermal spraying processes, such as APS (from 23 MPa to 40 MPa) [18,41,42,51], HVOF (from 20 MPa to 40 MPa) [45], AAPS (38.2 MPa) [52], as well as slightly higher than the values obtained by VPS (42 MPa) [18].

The stability of the Ti/HA coating was analyzed after 4 weeks of immersion in SBF solution. The tensile bond strength slightly decreased ( $55 \pm 5$  MPa) without statistically significance differences compared to non-immersed samples ( $p > 0.05$ ).

#### **3.4. Morphological changes upon immersion in Hank's solution**

Figure 5 shows the surface morphology of the Ti-HA coating after 1, 4 and 7 days of immersion in the Hank's solution and the release of calcium and phosphate ions. HA could be mainly observed at the valleys of the surface topography over the surface. This means that, by immersion, the dissolution and precipitation processes take place mainly at those sites, which may stimulate the bone ingrowth. Interestingly, some biomimetic apatite particles could be observed in higher magnification images.



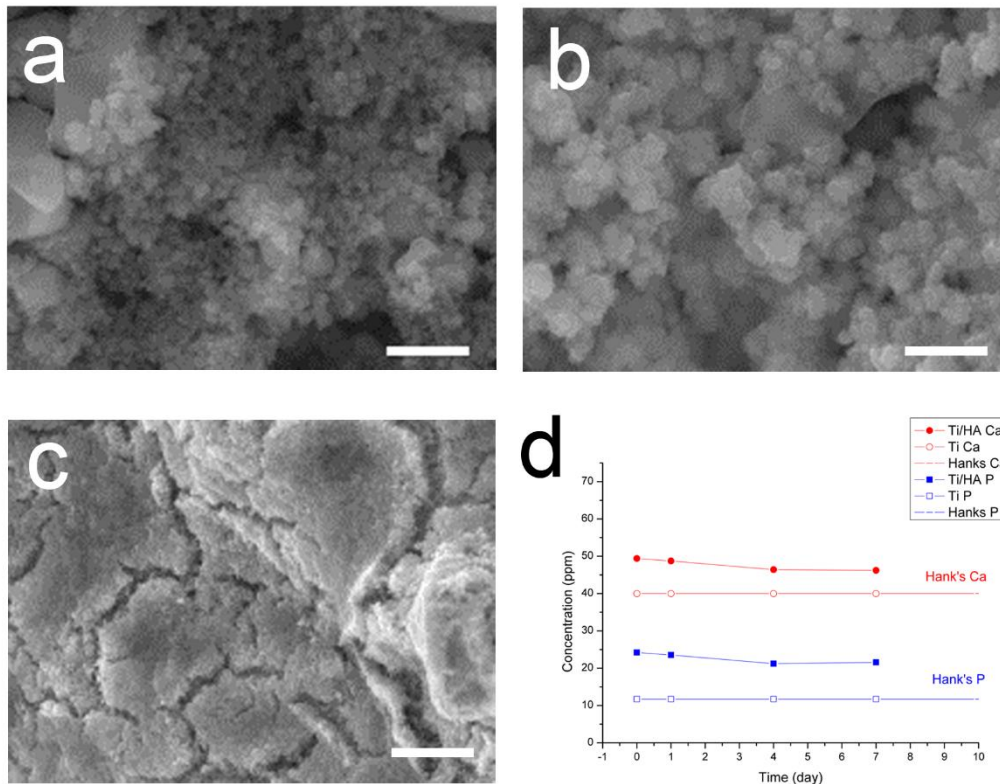


**Figure 5.** Morphology of Ti-HA coatings after immersing in Hank's solution and release of calcium and phosphate ions. Representative SEM images after 1 day (a), 4 days (b) and 7 days (b) of immersion. Scale bar denotes 1  $\mu\text{m}$ . Release of calcium (Ca) and phosphate (P) ions from Ti and Ti-HA coatings during the time of immersion (d).

After 4 days of immersion, the biomimetic apatite layer grew considerably on the Ti-HA coatings (Figure 5b). The growth of such layer with a very fine structure results from the complex dissolution-precipitation behavior [11,53]. After 7 days, the structure was preserved but the thickness of the apatite layer increased. Manipulation of the samples during dehydration and/or sputter coating may be the responsible for drying shrinkage and surface crack formation (Figure 5c).

Figure 5d shows the evolution of Ca and Pi release during the time of immersion in Hank's solution. An increase of both calcium and phosphate concentrations in the solution after one day of immersion of Ti-HA coated substrates was observed, which indicates dissolution of ions from the coating. Afterwards, calcium and phosphate concentration slightly decreased and kept approximately constant during the immersion, which would indicate a balance between precipitation/dissolution. In contrast, both calcium and phosphate ions maintained constant during the time of immersion and with the same levels than Hank's solution concentrations.

### **3.5. Phase identification of the coatings**

XRD results (Figure 6) show that, for both types of CGS coatings, the main phases of the coatings were practically the same than the feedstock powders, i.e. pristine HA and (Ti). However, some small peaks appeared that were attributed to oxide titanium phases, such as rutile and anatase ( $\text{TiO}_2$ ) as well as TiO, although the low intensity of both peaks indicate limited amount of these phases. The formation of  $\text{TiO}_2$  phase is generally caused by spontaneous oxidation of titanium and titanium alloys in contact with air, while the appearance of TiO could be attributed to the  $\text{TiO}_2$  reduction by Ti in an oxygen deficient atmosphere [45,54].

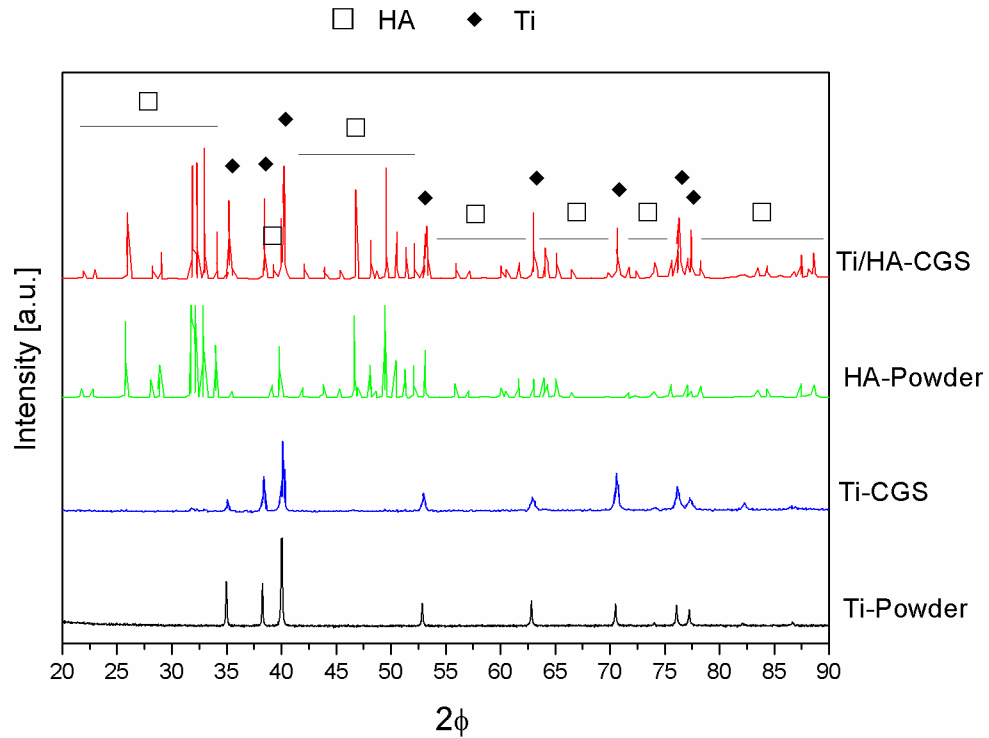


**Figure 6.** X-ray diffraction pattern of Ti powder, HA powder, Ti coating (Ti-CGS) and Ti-HA coating (Ti/HA-CGS).

In addition, the peak intensity of the two main phases was reduced and their peak width was broadened after spraying process of the Ti-HA powders. The slightly peak broadening could be explained by the refining of initial feedstock powders due to the fact that particles might be crushed during spraying [55]. Big broad bands were not observed due to the absence of amorphous phases produced by the thermal degradation of HA and Ti during CGS spraying. Noteworthy, TiO and TiO<sub>2</sub> phases were detected in feedstock powders, but no growth of titanium oxide peak intensity was detected on as sprayed Ti/HA CS coatings. In this same regard, CaO phase has not been identified neither on the feedstock powder nor over sprayed Ti-HA coatings.

### 3.6. Biological characterization

The percentage of cell viability after 24 h of incubation with different dilutions of medium is shown in Figure 7A.

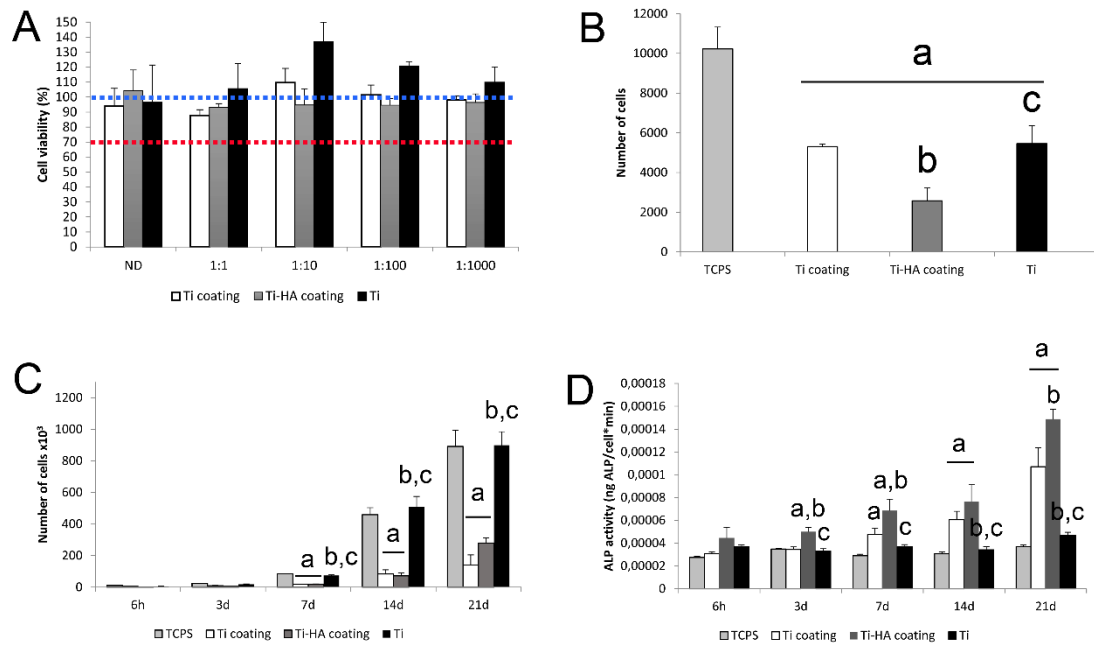


**Figure 7.** SaOS-2 cell behavior on the different analyzed surfaces. (A) Percentage of SaOS-2 cell viability after 24 h of exposure with different extract dilutions. Red line shows the limit of toxicity and blue line represents the optimal value. ND means non-diluted concentration. (B) Number of SaOS-2 cells after 6 h of cell adhesion on the different substrates. (C) SaOS-2 cell proliferation on the different substrates. (D) ALP activity of SaOS-2 cells cultured on the different substrates. In each figure, “a” means statistically significant differences ( $p < 0.05$ ) compared to TCPS, “b” means statistically significant differences compared to Ti coating and “c” means statistically significant differences compared to Ti-HA coating.

The percentage of cell viability in all the tested conditions was above 90% demonstrating no cytotoxic effects. The number of cells attached to Ti and Ti coatings were very similar, having approximately half of the seeded cells (Figure 7B). Similar results were obtained in previous works where titanium was coated through thermal spraying techniques [56,57]. Surprisingly, the number of cells seeded on Ti-HA was reduced to 25% compared to TCPS. This may be attributed to the elevated roughness obtained after spraying both Ti and HA, since HA coatings obtained through other strategies have been demonstrated to induce cellular adhesion [58,59]. Although this roughness could be detrimental for cellular adhesion it is expected that would be beneficial for osteointegration and mechanical fixation of the implant [60–62].

Proliferation assay showed a continuously increase of cell number over time on control Ti samples presenting similar levels than TCPS. In contrast, cells seeded on Ti and Ti-HA coated surfaces slowly increased during the cell culture periods studied (Figure 7C). This delayed increase may indicate that cells are differentiating into osteoblasts, since this process induces cell growth arrest [63]. Simultaneously to such process, a sequential and selective expression of genes is activated resulting in the differentiation into osteoblast lineage [64]. In the present work, both CGS Ti and Ti-HA coatings exhibited significantly higher ALP activity values compared to non-coated Ti and TCPS (Figure 7D). These higher values imply that probably surface topography is playing a significant role in the differentiation of SaOS-2 cells. Noteworthy, when surfaces were sprayed with Ti-HA composite highest ALP activity values at each time point were obtained. Therefore, presence of HA crystals on the Ti surface may play a synergistic effect on cell differentiation [65].

The interaction of cells with the different surfaces was also visualized by FESEM, showing cells completely spread on Ti control surfaces with very few protrusions (Figure

8a and 8b). In contrast, cells cultured on both Ti (Figure 8c and 8d) and Ti-HA (Figure 8e and 8f) coated surfaces presented an elongated shape with huge quantity of filopodia. Interestingly, in Ti-HA coated surfaces these cytoplasmic projections interacted directly with HA particles probably sensing them as chemotropic cues. This behavior has been previously observed on nanocrystalline HA coatings and has been related to preference of cells for nanostructured surfaces [66,67].

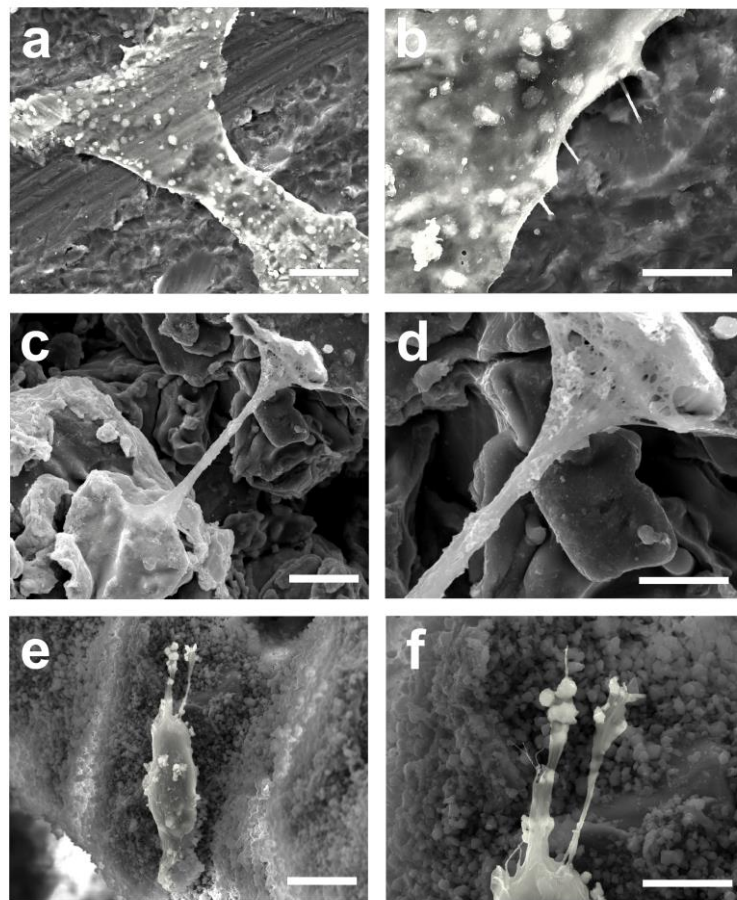


**Figure 8.** Cell morphology on Ti (a,b), Ti coated (c,d) and Ti-HA coated (e,f) surfaces at low (a,c,e; x2300) and high (b,d,f; x6000) magnification. Bar denotes 10  $\mu\text{m}$  (a,c,e) or 5  $\mu\text{m}$  (b,d,f).

## **Conclusions**

A Ti-HA coating presenting high porosity have been successfully obtained on Ti surface by CGS. The main advantage of this method is the low temperature achieved, which decreased the probability of titanium and/or calcium oxidation and undesirable formation of secondary metastable and/or amorphous HA phases. In this regard, use of this methodology opens the possibility to coat Ti surfaces with desired calcium phosphates formulations without any phase change during the process. In addition, adhesion and bond strength values obtained in the present work ensure long stability of the coatings obtained by CGS. Finally, the novel Ti-HA coating could be a promising candidate for bone applications due to the observed cellular response, especially in terms of osteoblastic cell differentiation.

## **4. ACKNOWLEDGEMENTS**

This work was supported by the Spanish Government through project MAT2015-67183-R, cofounded by the EU through the European Regional Development Funds. The authors acknowledge also the Generalitat de Catalunya for funding the project 2017SGR-1165 and for the ICREA Award of M-P Ginebra.

## **5. REFERENCES**

- [1] R.B. Heimann, Structure, properties, and biomedical performance of osteoconductive bioceramic coatings, *Surf. Coatings Technol.* 233 (2013) 27–38. doi:10.1016/j.surfcoat.2012.11.013.
- [2] S. Kurtz, K. Ong, E. Lau, F. Mowat, M. Halpern, Projections of primary and revision hip and knee arthroplasty in the United States from 2005 to 2030, *J. Bone Jt. Surg.* 89 (2007) 780–5. doi:10.2106/JBJS.F.00222.

- [3] M. Geetha, A.K. Singh, R. Asokamani, A.K. Gogia, Ti based biomaterials, the ultimate choice for orthopaedic implants - A review, *Prog. Mater. Sci.* 54 (2009) 397–425. doi:10.1016/j.pmatsci.2008.06.004.
- [4] D.R. Sumner, T.M. Turner, R. Igloria, R.M. Urban, J.O. Galante, Functional adaptation and ingrowth of bone vary as a function of hip implant stiffness, *J. Biomech.* 31 (1998) 909–917. doi:10.1016/S0021-9290(98)00096-7.
- [5] L. Lin, H. Wang, M. Ni, Y. Rui, T.-Y. Cheng, C.-K. Cheng, X. Pan, G. Li, C. Lin, Enhanced osteointegration of medical titanium implant with surface modifications in micro/nanoscale structures, *J. Orthop. Transl.* 2 (2014) 35–42. doi:10.1016/j.jot.2013.08.001.
- [6] W. Singhatanadgit, Biological Responses to New Advanced Surface Modifications of Endosseous Medical Implants, *Bone Tissue Regen. Insights.* 2 (2009) 1–11. doi:10.4137/BTRIS3150.
- [7] R.A. Surmenev, M.A. Surmeneva, A.A. Ivanova, Significance of calcium phosphate coatings for the enhancement of new bone osteogenesis - A review, *Acta Biomater.* 10 (2014) 557–579. doi:10.1016/j.actbio.2013.10.036.
- [8] J.P. Collier, V.A. Surprenant, M.B. Mayor, M. Wrona, R.E. Jensen, H.P. Surprenant, Loss of hydroxyapatite coating on retrieved, total hip components., *J. Arthroplasty.* 8 (1993) 389–93. doi:10.1016/S0883-5403(06)80037-9.
- [9] T. Reiner, I. Gotman, Biomimetic calcium phosphate coating on Ti wires versus flat substrates: Structure and mechanism of formation, *J. Mater. Sci. Mater. Med.* 21 (2010) 515–523. doi:10.1007/s10856-009-3906-y.



- [10] T. Li, J. Lee, T. Kobayashi, H. Aoki, Hydroxyapatite coating by dipping method, and bone bonding strength, *J. Mater. Sci. Mater. Med.* 7 (1996) 355–357.  
doi:10.1007/BF00154548.
- [11] M. Metikoš-Huković, E. Tkalacec, A. Kwokal, J. Piljac, An in vitro study of Ti and Ti-alloys coated with sol-gel derived hydroxyapatite coatings, *Surf. Coatings Technol.* 165 (2003) 40–50. doi:10.1016/S0257-8972(02)00732-6.
- [12] Y. Han, T. Fu, J. Lu, K. Xu, Characterization and stability of hydroxyapatite coatings prepared by an electrodeposition and alkaline-treatment process, *J. Biomed. Mater. Res.* 54 (2001) 96–101. doi:10.1002/1097-4636(200101)54:1<96::AID-JBM11>3.0.CO;2-U.
- [13] B.D. Hahn, J.M. Lee, D.S. Park, J.J. Choi, J. Ryu, W.H. Yoon, B.K. Lee, D.S. Shin, H.E. Kim, Mechanical and in vitro biological performances of hydroxyapatite-carbon nanotube composite coatings deposited on Ti by aerosol deposition, *Acta Biomater.* 5 (2009) 3205–3214.  
doi:10.1016/j.actbio.2009.05.005.
- [14] W.J.E.M. Habraken, J. Tao, L.J. Brylka, H. Friedrich, L. Bertinetti, A.S. Schenk, A. Verch, V. Dmitrovic, P.H.H. Bomans, P.M. Frederik, J. Laven, P. van der Schoot, B. Aichmayer, G. de With, J.J. DeYoreo, N.A.J.M. Sommerdijk, Ion-association complexes unite classical and non-classical theories for the biomimetic nucleation of calcium phosphate, *Nat. Commun.* 4 (2013) 1507.  
doi:10.1038/ncomms2490.
- [15] S.J. Ding, Properties and immersion behavior of magnetron-sputtered multi-layered hydroxyapatite/titanium composite coatings, *Biomaterials.* 24 (2003)

4233–4238. doi:10.1016/S0142-9612(03)00315-6.

- [16] J.M. Choi, H.E. Kim, I.S. Lee, Ion-beam-assisted deposition (IBAD) of hydroxyapatite coating layer on Ti-based metal substrate, *Biomaterials*. 21 (2000) 469–473. doi:10.1016/S0142-9612(99)00186-6.
- [17] L. Clèries, E. Martínez, J.M. Fernández-Pradas, G. Sardin, J. Esteve, J.L. Morenza, Mechanical properties of calcium phosphate coatings deposited by laser ablation, *Biomaterials*. 21 (2000) 967–971. doi:10.1016/S0142-9612(99)00240-9.
- [18] R. Gadow, A. Killinger, N. Stiegler, Hydroxyapatite coatings for biomedical applications deposited by different thermal spray techniques, *Surf. Coatings Technol.* 205 (2010) 1157–1164. doi:10.1016/j.surfcoat.2010.03.059.
- [19] N.W. Khun, Z. Li, K.A. Khor, J. Cizek, Higher in-flight particle velocities enhance in vitro tribological behavior of plasma sprayed hydroxyapatite coatings, *Tribol. Int.* 103 (2016) 496–503. doi:10.1016/j.triboint.2016.08.006.
- [20] H. Podlesak, L. Pawlowski, J. Laureyns, R. Jaworski, T. Lampke, Advanced microstructural study of suspension plasma sprayed titanium oxide coatings, *Surf. Coatings Technol.* 202 (2008) 3723–3731. doi:10.1016/j.surfcoat.2008.01.017.
- [21] S. Beauvais, V. Guipont, F. Borit, M. Jeandin, M. Espanol, K.A. Khor, A. Robisson, R. Saenger, Process-microstructure-property relationships in controlled atmosphere plasma spraying of ceramics, *Surf. Coatings Technol.* 183 (2004) 204–211. doi:10.1016/j.surfcoat.2003.08.078.

- [22] H. Singh, B.S. Sidhu, D. Puri, S. Prakash, Use of plasma spray technology for deposition of high temperature oxidation/corrosion resistant coatings - A review, *Mater. Corros.* 58 (2007) 92–102. doi:10.1002/maco.200603985.
- [23] R.S. Lima, K.A. Khor, H. Li, P. Cheang, B.R. Marple, HVOF spraying of nanostructured hydroxyapatite for biomedical applications, *Mater. Sci. Eng. A.* 396 (2005) 181–187. doi:10.1016/j.msea.2005.01.037.
- [24] Y. Huang, L. Song, X. Liu, Y. Xiao, Y. Wu, J. Chen, F. Wu, Z. Gu, Hydroxyapatite coatings deposited by liquid precursor plasma spraying: Controlled dense and porous microstructures and osteoblastic cell responses, *Biofabrication.* 2 (2010). doi:10.1088/1758-5082/2/4/045003.
- [25] R.B. Heimann, T.A. Vu, Low-pressure plasma-sprayed (LPPS) bioceramic coatings with improved adhesion strength and resorption resistance, *J. Therm. Spray Technol.* 6 (1997) 145–149. doi:10.1007/s11666-997-0005-9.
- [26] B.J. McEntire, B.S. Bal, M.N. Rahaman, J. Chevalier, G. Pezzotti, Ceramics and ceramic coatings in orthopaedics, *J. Eur. Ceram. Soc.* 35 (2015) 4327–4369. doi:10.1016/j.jeurceramsoc.2015.07.034.
- [27] F. Velard, J. Braux, J. Amedee, P. Laquerriere, Inflammatory cell response to calcium phosphate biomaterial particles: An overview, *Acta Biomater.* 9 (2013) 4956–4963. doi:10.1016/j.actbio.2012.09.035.
- [28] S. Bauer, P. Schmuki, K. von der Mark, J. Park, Engineering biocompatible implant surfaces. Part I: Materials and surfaces, *Prog. Mater. Sci.* (2012). doi:10.1016/j.pmatsci.2012.09.001.

- [29] A.C.W. Noorakma, H. Zuhailawati, V. Aishvarya, B.K. Dhindaw, Hydroxyapatite-coated magnesium-based biodegradable alloy: Cold spray deposition and simulated body fluid studies, *J. Mater. Eng. Perform.* 22 (2013) 2997–3004. doi:10.1007/s11665-013-0589-9.
- [30] a Choudhuri, P.S. Mohanty, J. Karthikeyan, Bio-ceramic composite coatings by cold spray technology, *Proc. Int. Therm. Spray Conf.* (2009) 391–396. doi:10.1361/cp2009itsc0391.
- [31] D. Qiu, M. Zhang, L. Grøndahl, A novel composite porous coating approach for bioactive titanium-based orthopedic implants, *J. Biomed. Mater. Res. - Part A.* 101 A (2013) 862–872. doi:10.1002/jbm.a.34372.
- [32] M. Gardon, A. Concustell, S. Dosta, N. Cinca, I.G. Cano, J.M. Guilemany, Improved bonding strength of bioactive cermet Cold Gas Spray coatings, *Mater. Sci. Eng. C.* 45 (2014) 117–121. doi:10.1016/j.msec.2014.08.053.
- [33] N. Cinca, A.M. Vilardell, S. Dosta, A. Concustell, I. Garcia Cano, J.M. Guilemany, S. Estradé, A. Ruiz, F. Peiró, A New Alternative for Obtaining Nanocrystalline Bioactive Coatings: Study of Hydroxyapatite Deposition Mechanisms by Cold Gas Spraying, *J. Am. Ceram. Soc.* 99 (2016) 1420–1428. doi:10.1111/jace.14076.
- [34] American Society of Testing Materials, ASTM E3 Standard Guide for Preparation of Metallographic Specimens, ASTM Copyright. i (2011) 1–12. doi:10.1520/E0003-11.2.
- [35] AMERICAN SOCIETY FOR TESTING AND MATERIALS, ASTM C633–13, Stand. Test Method Adhes. or Cohes. Strength Therm. Spray Coatings. 3 (2017)

1–7. doi:10.1520/C0633-13.Copyright.

- [36] International Organization for Standardization, Biological Evaluation of Medical Devices Part 5: Tests for In Vitro Cytotoxicity, Iso 10993–5. 5 (2009) 1–52.
- [37] H.E. Exner, C. Müller, Particle rearrangement and pore space coarsening during solid-state sintering, in: *J. Am. Ceram. Soc.*, 2009: pp. 1384–1390.  
doi:10.1111/j.1551-2916.2009.02978.x.
- [38] H. Melero, G. Fargas, N. Garcia-Giralt, J. Fernández, J.M. Guilemany, Mechanical performance of bioceramic coatings obtained by high-velocity oxy-fuel spray for biomedical purposes, *Surf. Coatings Technol.* 242 (2014) 92–99.  
doi:10.1016/j.surfcoat.2014.01.023.
- [39] L. Sun, C.C. Berndt, K.A. Khor, H.N. Cheang, K.A. Gross, Surface characteristics and dissolution behavior of plasma-sprayed hydroxyapatite coating, *J. Biomed. Mater. Res.* 62 (2002) 228–236. doi:10.1002/jbm.10315.
- [40] H.C. Man, N.Q. Zhao, Z.D. Cui, Surface morphology of a laser surface nitrided and etched Ti-6Al-4V alloy, *Surf. Coatings Technol.* 192 (2005) 341–346.  
doi:10.1016/j.surfcoat.2004.07.076.
- [41] K.A. Khor, Y.W. Gu, C.H. Quek, P. Cheang, Plasma spraying of functionally graded hydroxyapatite/Ti-6Al-4V coatings, *Surf. Coatings Technol.* 168 (2003) 195–201. doi:10.1016/S0257-8972(03)00238-X.
- [42] G. Zhao, L. Xia, G. Wen, L. Song, X. Wang, K. Wu, Microstructure and properties of plasma-sprayed bio-coatings on a low-modulus titanium alloy from milled HA/Ti powders, *Surf. Coatings Technol.* 206 (2012) 4711–4719.

doi:10.1016/j.surfcoat.2011.08.033.

- [43] Y.C. Yang, C.Y. Yang, Mechanical and histological evaluation of a plasma sprayed hydroxyapatite coating on a titanium bond coat, *Ceram. Int.* 39 (2013) 6509–6516. doi:10.1016/j.ceramint.2013.01.083.
- [44] E. Mohseni, E. Zalnezhad, A.R. Bushroa, Comparative investigation on the adhesion of hydroxyapatite coating on Ti-6Al-4V implant: A review paper, *Int. J. Adhes. Adhes.* 48 (2014) 238–257. doi:10.1016/j.ijadhadh.2013.09.030.
- [45] X. Zhou, R. Siman, L. Lu, P. Mohanty, Argon atmospheric plasma sprayed hydroxyapatite/Ti composite coating for biomedical applications, *Surf. Coatings Technol.* 207 (2012) 343–349. doi:10.1016/j.surfcoat.2012.07.009.
- [46] S.W.K. Kweh, K.A. Khor, P. Cheang, Plasma-sprayed hydroxyapatite (HA) coatings with flame-spheroidized feedstock: Microstructure and mechanical properties, *Biomaterials.* 21 (2000) 1223–1234. doi:10.1016/S0142-9612(99)00275-6.
- [47] X. Zheng, M. Huang, C. Ding, Bond strength of plasma-sprayed hydroxyapatite/Ti composite coatings, *Biomaterials.* 21 (2000) 841–849. doi:10.1016/S0142-9612(99)00255-0.
- [48] Y.C. Yang, E. Chang, The bonding of plasma-sprayed hydroxyapatite coatings to titanium: Effect of processing, porosity and residual stress, *Thin Solid Films.* 444 (2003) 260–275. doi:10.1016/S0040-6090(03)00810-1.
- [49] H. Li, K.A. Khor, P. Cheang, Adhesive and bending failure of thermal sprayed hydroxyapatite coatings: Effect of nanostructures at interface and crack

- propagation phenomenon during bending, *Eng. Fract. Mech.* 74 (2007) 1894–1903. doi:10.1016/j.engfracmech.2006.06.001.
- [50] Y.W. Gu, K.A. Khor, P. Cheang, In vitro studies of plasma-sprayed hydroxyapatite/Ti-6Al-4V composite coatings in simulated body fluid (SBF), *Biomaterials*. 24 (2003) 1603–1611. doi:10.1016/S0142-9612(02)00573-2.
- [51] J. Fernández, M. Gaona, J.M. Guilemany, Effect of heat treatments on HVOF hydroxyapatite coatings, *J. Therm. Spray Technol.* 16 (2007) 220–228. doi:10.1007/s11666-007-9034-7.
- [52] S.H. Zahiri, C.I. Antonio, M. Jahedi, Elimination of porosity in directly fabricated titanium via cold gas dynamic spraying, *J. Mater. Process. Technol.* 209 (2009) 922–929. doi:10.1016/j.jmatprotec.2008.03.005.
- [53] P. Li, K. de Groot, Better bioactive ceramics through sol-gel process - Code: G2, *J. Sol-Gel Sci. Technol.* 2 (1994) 797–801. doi:10.1007/BF00486353.
- [54] H. Poelman, H. Tomaszewski, D. Poelman, D. Depla, R. De Gryse, Effect of the oxygen deficiency of ceramic TiO<sub>2-x</sub> targets on the deposition of TiO<sub>2</sub> thin films by DC magnetron sputtering, in: *Surf. Interface Anal.*, 2004: pp. 1167–1170. doi:10.1002/sia.1867.
- [55] L. Sun, C.C. Berndt, C.P. Grey, Phase, structural and microstructural investigations of plasma sprayed hydroxyapatite coatings, *Mater. Sci. Eng. A*. 360 (2003) 70–84. doi:10.1016/S0921-5093(03)00439-8.
- [56] T.J. Webster, C. Ergun, R.H. Doremus, W. a Lanford, Increased osteoblast adhesion on titanium-coated hydroxylapatite that forms CaTiO<sub>3</sub>., *J. Biomed.*

- Mater. Res. A. 67 (2003) 975–980. doi:10.1002/jbm.a.10160.
- [57] M.D. Ball, S. Downes, C.A. Scotchford, E.N. Antonov, V.N. Bagratashvili, V.K. Popov, W.J. Lo, D.M. Grant, S.M. Howdle, Osteoblast growth on titanium foils coated with hydroxyapatite by pulsed laser ablation, *Biomaterials*. 22 (2001) 337–347. doi:10.1016/S0142-9612(00)00189-7.
- [58] J. Harle, H.W. Kim, N. Mordan, J.C. Knowles, V. Salih, Initial responses of human osteoblasts to sol-gel modified titanium with hydroxyapatite and titania composition, *Acta Biomater.* 2 (2006) 547–556. doi:10.1016/j.actbio.2006.05.005.
- [59] C. Caparrós, M. Ortiz-Hernandez, M. Molmeneu, M. Punset, J.A. Calero, C. Aparicio, M. Fernández-Fairén, R. Perez, F.J. Gil, Bioactive macroporous titanium implants highly interconnected, *J. Mater. Sci. Mater. Med.* 27 (2016). doi:10.1007/s10856-016-5764-8.
- [60] J.Y. Martin, Z. Schwartz, T.W. Hummert, D.M. Schraub, J. Simpson, J. Lankford, D.D. Dean, D.L. Cochran, B.D. Boyan, Effect of titanium surface roughness on proliferation, differentiation, and protein synthesis of human osteoblast-like cells (MG63), *J. Biomed. Mater. Res.* 29 (1995) 389–401. doi:10.1002/jbm.820290314.
- [61] B.D. Boyan, R. Batzer, K. Kieswetter, Y. Liu, D.L. Cochran, S. Szmuckler-Moncler, D.D. Dean, Z. Schwartz, Titanium surface roughness alters responsiveness of MG63 osteoblast-like cells to 1  $\alpha$ ,25-(OH) $_2$ D $_3$ , *J. Biomed. Mater. Res.* 39 (1998) 77–85. doi:10.1002/(SICI)1097-4636.
- [62] Y. Wu, J.P. Zitelli, K.S. TenHuisen, X. Yu, M.R. Libera, Differential response of



- Staphylococci and osteoblasts to varying titanium surface roughness, *Biomaterials*. 32 (2011) 951–960. doi:10.1016/j.biomaterials.2010.10.001.
- [63] R.T. Franceschi, The Developmental Control of Osteoblast-Specific Gene Expression: Role of Specific Transcription Factors and the Extracellular Matrix Environment, *Crit. Rev. Oral Biol. Med.* 10 (1999) 40–57. doi:10.1177/10454411990100010201.
- [64] K. Nakashima, B. De Crombrughe, Transcriptional mechanisms in osteoblast differentiation and bone formation, *Trends Genet.* 19 (2003) 458–466. doi:10.1016/S0168-9525(03)00176-8.
- [65] Aniket, R. Reid, B. Hall, I. Marriott, A. El-Ghannam, Early osteoblast responses to orthopedic implants: Synergy of surface roughness and chemistry of bioactive ceramic coating, *J. Biomed. Mater. Res. - Part A*. 103 (2015) 1961–1973. doi:10.1002/jbm.a.35326.
- [66] Z. Shi, X. Huang, Y. Cai, R. Tang, D. Yang, Size effect of hydroxyapatite nanoparticles on proliferation and apoptosis of osteoblast-like cells, *Acta Biomater.* 5 (2009) 338–345. doi:10.1016/j.actbio.2008.07.023.
- [67] M. Sato, M.A. Sambito, A. Aslani, N.M. Kalkhoran, E.B. Slamovich, T.J. Webster, Increased osteoblast functions on undoped and yttrium-doped nanocrystalline hydroxyapatite coatings on titanium, *Biomaterials*. 27 (2006) 2358–2369. doi:10.1016/j.biomaterials.2005.10.041.